hydrogen

MDPI

Article

Investigation of the Hydrogen Absorption by the $LaNi_5$ and $LaNi_{4.75}Pb_{0.25}$ Alloys Using a Statistical Physics Model

Michał Żurek * and Wojciech Zając

The Henryk Niewodniczański Institute of Nuclear Physics Polish Academy of Sciences, Radzikowskiego 152, 31-342 Cracow, Poland

* Correspondence: michal.zurek@ifj.edu.pl

Abstract: A theoretical model was selected among three potentially applicable models and then used to analyze the absorption isotherms of the hydrogen storage alloys $LaNi_5$ and $LaNi_{4.75}Pb_{0.25}$ at three different temperatures (T = 303 K, 313 K, 323 K). The theoretical expressions of the model were based on the statistical physics formalism and simplifying hypotheses. The model selected was the one with the highest correlation with the experimental data. The model had six adjustable parameters: the number of hydrogen atoms per site n_α, n_β, the receptor site densities N_α, N_β and the energy parameters P_α, P_β. The fitted parameters obtained for the Pb-doped and nondoped alloys were compared and discussed in relationship to the absorption isotherms. Finally, the fitted parameters or the model were further applied to calculate thermodynamic functions, such as entropy, Gibbs free energy and internal energy, which govern the absorption mechanism.

Keywords: hydrogen absorption isotherms; statistical physics model; grand canonical ensemble

Citation: Żurek, M.; Zając, W. Investigation of the Hydrogen Absorption by the $LaNi_5$ and $LaNi_{4.75}Pb_{0.25}$ Alloys Using a Statistical Physics Model. *Hydrogen* **2022**, *3*, 361–378. https://doi.org/10.3390/hydrogen3030022

Academic Editors: Jacques Huot, Fusheng Yang and Giovanni Capurso

Received: 21 July 2022
Accepted: 7 September 2022
Published: 15 September 2022

1. Introduction

Metal hydrides MH are formed by the reversible reaction of hydrogen with metals or their alloys. For some metals, the absorption reaction occurs at room temperature and at relatively low hydrogen pressures [1,2]. For most metallic hydrides, high density of hydrogen accumulation has been achieved. Thanks to their ability to absorb large amounts of hydrogen in a small volume, metal hydrides can be considered as potential materials for hydrogen storage—especially in applications where the weight of containers is not critical.

The metal hydrides dedicated for hydrogen storage applications are expected to exhibit a high storage capacity, reversibility and long-term stability. Among others, the intermetallic compounds derived from $LaNi_5$ (general formula AB_5) have been extensively investigated for many years as possible hydrogen storage materials [1–3]. One of the methods to improve the hydrogen absorption properties of $LaNi_5$ is to replace La, Ni or both by other elements: La by Ce, Pr, Nd or by a mischmetal and Ni by Pb, Zn, Cr, Fe, Co, Cu or even by Al or Sn. Replacing Ni by other elements can improve the long-term stability and resistance of a hydride to hydrogen impurity.

Experimental *pcT* (pressure–composition–temperature) measurements can deliver information about the macroscopic state of a tested hydride, e.g., the maximum storage capacity, reversibility of a process or long-term stability. Earlier works [1,2] have shown that there is a correlation between the crystallographic and thermodynamic properties of hydrides and the hydrogen concentration in them. This provides a useful starting point for further theoretical studies.

Theoretical investigations based on statistical physics models can be treated as complementary to experimental research as they can provide characteristics of the microscopic state of a hydride. It is then possible to unveil the mechanism of hydrogen distribution in hydrides and to determine the evolution of thermodynamic functions, e.g., internal energy E_{int}, Gibbs free energy G_a and entropy S_a, basing on theoretical models.

There are many models which employ the statistical physics methods to describe the behavior of real metal hydride systems. Such models were proposed, developed and successfully used by several authors [4–9] to characterize metal hydrides. A common feature of all those models is methodology which includes numerically fitting the analytical expressions to the previously known experimental *pcT* isotherms and looking for correlations between them.

The aim of this paper is to apply a theoretical model to the hydrogen absorption isotherms and then to derive and analyze the thermodynamic characteristics of hydrides created of the well known $LaNi_5$ alloy [1,2] as well as of a poorly described in literature hydride of Pb-doped alloy $LaNi_{4.75}Pb_{0.25}$ [3]. The hydride of this Pb-doped alloy has been—probably for the first time—introduced in paper [3]. Finally, according to the proposed model, to study the influence of Pb doping of a base alloy at a molecular level.

2. Materials and Methods

The $LaNi_5$ and $LaNi_{4.75}Pb_{0.25}$ alloys were obtained by arc melting of high purity elements La (99.5%), Ni (99.9%) and Pb (99.99%) in the required mass ratios under 0.8 bar Ar atmosphere. The previous experience in the preparation of the AB_5 alloys showed an intensive evaporation of components—mainly Ni—during the melting process. In order to compensate for the mass loss, and to maintain the stoichiometry of the alloy it was decided to use 5% mass excess of Ni.

After melting, the specimens were slowly cooled down to the room temperature and then annealed at 573 K for 8 h under dynamic vacuum. The homogeneity of the obtained samples were checked by the powder X-ray diffraction at room temperature using X'Pert PRO diffractometer with CuKα radiation.

The samples with high purity, i.e., with low or zero content of foreign phases, were selected for the activation procedure and finally for hydrogenation. The activation procedure included storing the samples at 398 K under hydrogen atmosphere at the continuously maintained pressure of 10 bar. After 96 h, the samples were slowly cooled to room temperature and subjected to multiple hydriding/dehydriding cycles. The hydriding/dehydriding cycling was repeated until the equilibrium pressure of hydrogen absorption reached the minimum value and hydrogen absorption capacity did not vary by more than 5% between successive cycles. Hence, it could be concluded that the samples had been fully activated and stable so that reproducible absorption *pcT* isotherms could be obtained. For $LaNi_5$ and $LaNi_{4.75}Pb_{0.25}$ alloys, the four and six complete hydriding/dehydriding cycles were required, respectively.

The evolution of the hydrogen absorption and desorption properties of these alloys was measured by the Sievert's volumetric method at T = 303 K, 313 K and 323 K, using commercial gas absorption analyzer Hiden Isochema IMI. For the measurements, samples with mass below 500 mg were used. In addition, it was ensured that the whole volume of the measurement sample holder was completely filled by the sample—without any voids, thereby maintaining close-packing of the powder sample grains. In this way, a thermal conductivity at the grains boundary and hydrogen diffusion rate could be improved. In addition no filler or thermal balance, such as high purity graphite powder, was used during the measurements. In the experiments, high purity grade (6.0) hydrogen gas was used.

The uncertainty of pressure measurement was equal to 0.05% of FSR (100 bar) and uncertainty of the absorbed hydrogen mass (including uncertainties of the sample mass, geometric dimensions of the reactor, hydrogen uptake, temperature stability) was estimated at 2.5 wt.%.

The *pcT* isotherms were taken at the above mentioned temperatures, as representing the most likely operating environment conditions for typical portable hydrogen tanks. The obtained results of the equilibrium pressure and absorption capacity for the $LaNi_5$ base and Pb-doped alloy do did not differ significantly from the data reported in other studies, e.g., for $LaNi_5$ [1,2] and $LaNi_{4.75}Pb_{0.25}$ [3] respectively.

Based on experimental hydrogen absorption data, the properties of hydrides, including their thermodynamic characteristics, have been determined and analyzed within the framework of three models derived from statistical physics. This work is limited to modelling the hydrogen absorption phenomenon, but the presented models can be successfully used also to the desorption process, which is the reverse of absorption.

3. Results

3.1. Theoretical Background and Model Details

The general reversible reaction of a hydrogen molecule with a metal alloy M, leading to the formation of metal hydride (MH_n), is expressed by Equation (1) [4–6]:

$$\frac{n}{2}H_2 + M \rightleftharpoons MH_n, \quad (1)$$

where n is a stoichiometric coefficient representing the number of H-atoms absorbed during reaction. The study of the hydrogen absorption processes in metal hydrides using the statistical physics method is expected to give the distribution of N_a hydrogen atoms absorbed onto N_m interstitial sites located in the unit mass of a hydride. The theoretical model requires assumptions listed below [4–9]:

- The hydrogen absorption materials are single phase alloys—supposed to be ideal, without any structural defects;
- The energy resulting during the formation of the hydride phase due to mechanical stresses of crystal structure is not taken into account at model approach;
- The investigated hydrides are considered as thermodynamic open systems, which can exchange both energy and matter with their surroundings. During the hydrogen absorption process by metal hydrides, hydrogen molecules pass from a gaseous state to the absorbed one. The reverse reaction occurs during the desorption process. Each direction of the hydrogen atoms/molecules flow is related to the absorption or release of heat. In the statistical approach, any process occurring in thermodynamic open systems can be described by the grand canonical ensemble (Equation (2)) [4–9].
- The next model assumption is related to hydrogen molecules, which are considered to constitute an ideal gas—a concept in the classical approximation with Maxwell–Boltzmann distribution. Based on this simplification, the interaction between hydrogen molecules in the gaseous state can be neglected. Internal gas energy can be determined by most important degrees of freedom [4–7,10]. From here, the energy of hydrogen molecules is fully characterized by their internal degrees of freedom, e.g., translation $\Delta\epsilon_t$, rotation $\Delta\epsilon_r$, vibration $\Delta\epsilon_v$, electronic $\Delta\epsilon_e$ and nuclear $\Delta\epsilon_n$, whose energies are related as follows $\Delta\epsilon_t \ll \Delta\epsilon_r \ll \Delta\epsilon_v \ll \Delta\epsilon_e \ll \Delta\epsilon_n$ [11].
  As long as the molecular gas temperature T (consequently energy, which is proportional to T), is lower than T_t ($T < \Delta T_r$), the rotational and vibrational degrees of freedom are not excited during collisions and the gas behaves as a simple monoatomic gas [11]. At higher temperatures, $T_r < T < T_v$, the rotational degrees of freedom become excited during gas molecules collisions, but oscillations remain frozen [11]. Finally, the electronic and nuclear degrees of freedom cannot be thermally activated at a reasonable temperature. They begin to play a role at high temperatures, e.g., $T_e \sim (10^4$–$10^5)$ K for electronic degrees of freedom and for $T_n \sim (10^7$–$10^8)$ K in case of nuclear [11]. Similarly, a vibration degree of freedom can be neglected compared to other ones [5–8].
  Finally, to simplify the statistical model, only the most important degrees of freedom which contribute to molecules energy at ambient temperatures are considered. For hydrogen, they are translational and rotational degrees of freedom.

The starting point of theoretical considerations is the grand canonical partition function (z_{gc}), Equation (2) [5,7,8], which defines the microscopic state of the system, depending on the physical situation the system is placed in.

$$z_{gc} = \sum_{N_i} e^{-\beta(\varepsilon_i - \mu)N_i}, \tag{2}$$

where ϵ_i and μ are the absorption energy per site and chemical potential of a site, respectively. The parameter N_i describes the occupation of a site and it can take two values: zero when a site is empty or unity if a site is filled by H-atoms. The β parameter is defined as $1/k_B T$, where k_B is the Boltzmann constant and T is the absolute temperature.

Assuming that all of the receptor sites N_M per unit absorbent mass are indistinguishable, which means that hydrogen atoms may be stored on each site with equal probability, the total grand canonical partition function $\left(Z_{gc}\right)$ can be expressed as Equation (3) [7,8]:

$$Z_{gc} = \left(z_{gc}\right)^{N_M}. \tag{3}$$

The average occupation N_a of the receptor sites by H-atoms is calculated using Equation (4) [4–10]:

$$N_a = k_B T \frac{\partial \ln\left(Z_{gc}\right)}{\partial \mu}. \tag{4}$$

3.2. Model with Two Absorption Energy Levels

Based on Equation (3), the model with two energy levels and variable numbers N_1 and N_2 of hydrogen atoms absorbed in two independent kinds of interstitial sites can be developed to calculate the amount of absorbed hydrogen versus pressure. For the purpose of this model (named Model 2), it was assumed that the number density of hydrogen absorption sites of the first type is N_α and that of the second type is N_β. The sites are characterized by the absorption energy values $-\epsilon_\alpha$ and $-\epsilon_\beta$, respectively. Consequently, the filling by hydrogen atoms of each type sites leads to the formations of two individual phases called α and β. The testing model can be treated as a simple topological issue. The total grand canonical partition function $\left(Z_{gc}\right)$ for this model is given by Equation (5) [4–10]:

$$Z_{gc} = \left(z_{gc\alpha}\right)^{N_\alpha} \left(z_{gc\beta}\right)^{N_\beta}, \tag{5}$$

where the grand canonical partition functions $z_{gc\alpha}$ and $z_{gc\beta}$ are related to the first and second site types, respectively, are expressed by Equations (6) and (7):

$$z_{gc\alpha} = \sum_{N_\alpha = 0,1} e^{-\beta(-\varepsilon_\alpha - \mu)N_\alpha} = 1 + e^{\beta(\varepsilon_\alpha + \mu)}, \tag{6}$$

$$z_{gc\beta} = \sum_{N_\beta = 0,1} e^{-\beta(-\varepsilon_\beta - \mu)N_\beta} = 1 + e^{\beta(\varepsilon_\beta + \mu)}. \tag{7}$$

The chemical potential μ_m is given by the equation $\mu_m = \mu/n$, where μ is the chemical potential of the site and n is the number of atoms per site. The chemical potential μ_m of a hydrogen molecule in the gaseous state is expressed by Equation (8) [4–8,10].

$$\mu_m = k_B T \ln\left(\frac{N}{Z_g}\right), \tag{8}$$

$$Z_g = z_{gtr} \cdot z_{grot}. \tag{9}$$

The partition function Z_g Equation (9) of a free hydrogen gas molecule can be expressed by partition functions of a translational Equation (10) rotational Equation (11) and vibrational degrees of freedom [7,8,10,11], where:

$$z_{gtr} = V\left(\frac{2\pi m k_B T}{h^2}\right)^{\frac{3}{2}}, \tag{10}$$

$$z_{grot} = \frac{T}{T_r}, \tag{11}$$

where m is the mass of the absorbed atom (1.00784 u), h is the Planck's constant and V is the volume of the studied system. The translation partition function per volume unit z_v, for an ideal gas, can be formulated versus the saturated vapor pressure P_{vs} and the vaporization energy ΔE_v as Equation (12) [5–8]:

$$P_{vs} = \left(\frac{2\pi m k_B T}{h^2}\right)^{\frac{3}{2}} k_B T \exp\left(\frac{-\Delta E^v}{RT}\right) \tag{12}$$

Using the canonical partition function given by Equation (5) and the expression from Equation (4), the average numbers N_1 and N_2 of occupied sites for α and β type are given by Equation (13) [7,8,10]:

$$N_1(P) = \frac{N_\alpha}{1 + \left(\frac{P_\alpha}{P}\right)^{n_\alpha}},\ N_2(P) = \frac{N_\beta}{1 + \left(\frac{P_\beta}{P}\right)^{n_\beta}} \tag{13}$$

where n_α and n_β are the numbers of hydrogen atoms per site, $P_\alpha = k_B T Z_g e^{-\beta\epsilon_\alpha}$ and $P_\beta = k_B T Z_g e^{-\beta\epsilon_\beta}$ are the pressures at half saturation respectively, for the α and β sites. According to Equation (4) and using the average site occupation N_1, N_2 derived by Equation (13) the average number of absorbed H-atoms N_a can be describe by Equation (14) [7,8]:

$$N_a = n_\alpha N_1 + n_\beta N_2. \tag{14}$$

Finally, combining Equations (13) and (14) the formula to express the amount of the absorbed hydrogen N_a as a function of pressure can be expressed by Equation (15) [7,8].

$$N_a(P) = N_1(P) + N_2(P) = n_\alpha \frac{N_\alpha}{1 + \left(\frac{P_\alpha}{P}\right)^{n_\alpha}} + n_\beta \frac{N_\beta}{1 + \left(\frac{P_\beta}{P}\right)^{n_\beta}}. \tag{15}$$

3.3. Model Adjustment and Validity

Three analytical models, most frequently used in literature to describe such systems are listed in Table 1 [7,8]. The selection of the appropriate model to fit the experimental data is made on a mathematical and physical level. The three applicable models have been tested by fitting them to the experimental hydrogen absorption isotherms of the $LaNi_5$ and $LaNi_{4.75}Pb_{0.25}$ alloys. The quality of a fit was checked based on the regression correlation coefficient R^2 and residual root mean square error RMSE—also known as the estimated standard error of the regression [4]. The fitted model is considered to show a good agreement with absorption isotherms if the regression coefficient R^2 is close to unity and the value of RMSE is close to zero.

Table 1. Partition functions of the tested models.

Name of Tested Model	Partition Function Z_{gc} Equation (2)
Model 1	$Z_{gc} = \left(1 + e^{\beta(\epsilon+\mu)}\right)^{N_\alpha}$
Model 2	$Z_{gc} = \left(1 + e^{\beta(\epsilon_\alpha+\mu)}\right)^{N_\alpha} \cdot \left(1 + e^{\beta(\epsilon_\beta+\mu)}\right)^{N_\beta}$
Model 3	$Z_{gc} = \left(1 + e^{\beta(\epsilon_\alpha+\mu)}\right)^{N_\alpha} \cdot \left(1 + e^{\beta(\epsilon_\beta+\mu)}\right)^{N_\beta} \cdot \left(1 + e^{\beta(\epsilon_\gamma+\mu)}\right)^{N_\gamma}$

The acceptable values of the correlation coefficients R^2 and RMSE (Table 2) were obtained for Model 2, assuming two energy levels ϵ_α and ϵ_β. From the physical point of view, the validation of models should be done in accordance with the real system properties, e.g., its crystallographic structure.

Many intermetallic AB_5 alloys including $LaNi_5$ and $LaNi_{4.75}Pb_{0.25}$, crystallize in the hexagonal $CaCu_5$ type structure with P_6/mmm space group [1,3]. The unit cell contains

one La atom in the Wyckoff $(1a)$ position and five Ni atoms located in two crystallographic positions. Two nickel atoms labeled Ni^1 are located in position $(2c)$ and three Ni atoms labeled Ni^2 in position $(3g)$.

In this structure there are capacious tetrahedral (Th) type interstitial site formed by La and Ni atoms e.g., Ni_4 $(4h)$, $LaNi_2Ni_2$ $(6m)$, $LaNi^{3g}Ni_2{}^{2c}$ $(12o)$, $LaNi_2{}^{3g}Ni^{2c}$ $(12n)$, and the octahedral (Oh) type site $La_2Ni_2{}^{2c}Ni_2{}^{3g}$ $(12n)$. The difference in interatomic distances and types of atoms creating the interstitial sites (Th) and (Oh) lead to their different hydrogen absorption energies ϵ and chemical potentials μ. For this reason, during absorption process the hydrogen atoms fill the above mentioned sites at two different absorption levels at different pressure values P_α and P_β. In consequence, two phases denoted as α and β appear during the overall process. The α phase is a solid solution of hydrogen in an alloy with low hydrogen concentrations ($\sim$0.1 wt.%) and the second phase β is a full metal hydride with the maximum hydrogen concentration ($\sim$1.2 wt.%).

These assumptions make Model 2 the most appropriate to describe intermetallic hydrides of the AB_5 type. The results obtained for this model are collected in Tables 2 and 3 and Figures 1 and 2. A slight misfit of the tested model in the low hydrogen concentration range (<0.1 wt.%) may be due to the effects of samples grains powdering [7].

Table 2. Values of the regression correlation coefficient R^2 and the residual root mean square error (RMSE) for the fit of Model 2 to the experimental absorption isotherms. The values xx/yy correspond to R^2/RMSE.

Temp K	$LaNi_5$	$LaNi_{4.75}Pb_{0.25}$
303	0.998/0.014	0.995/0.023
313	0.998/0.017	0.996/0.021
323	0.997/0.011	0.995/0.038

Table 3. Adjusted model parameter values for absorption processes according to the best fitting model (Model 2), where values xx/yy correspond to $LaNi_5$ and $LaNi_{4.75}Pb_{0.25}$, respectively.

Temp K	n_α	n_β	N_α	N_β	P_α	P_β
303	0.84/3.18	21.72/74.40	0.26/0.13	0.06/0.01	2.13/3.17	3.14/3.77
313	0.68/1.01	18.87/44.06	0.32/0.20	0.07/0.02	2.70/3.86	3.81/4.44
323	0.59/0.97	17.99/34.17	0.38/0.18	0.068/0.18	3.57/4.63	5.42/6.20

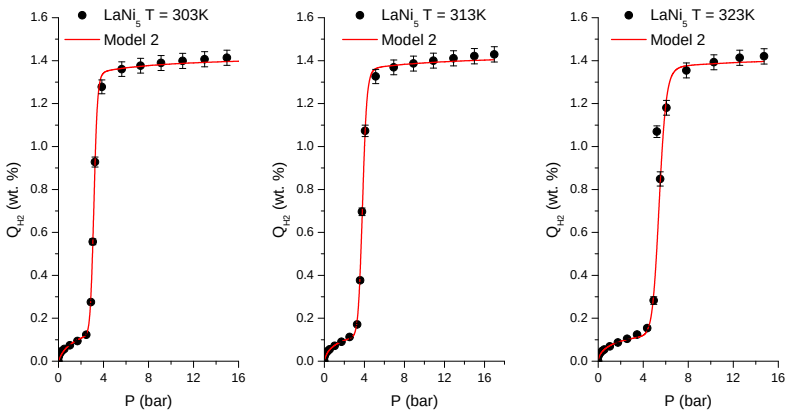

Figure 1. Hydrogen absorption isotherms for $LaNi_5$ at 303 K, 313 K, 323 K. The black circles are the experimental pcT data and the line is the simulation data obtained by using Model 2.

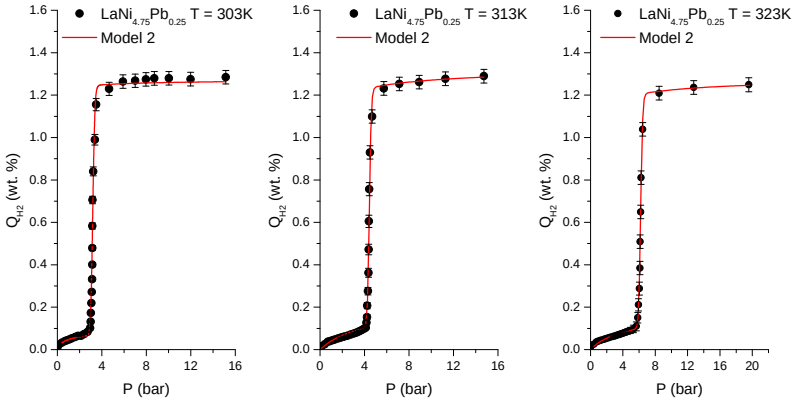

Figure 2. Hydrogen absorption isotherms for $LaNi_{4.75}Pb_{0.25}$ at 303 K, 313 K, 323 K. The black circles are the experimental *pcT* data and the line is the simulation data obtained by using Model 2.

The tested model (Model 2) with two types of interstitial sites contains six adjustable parameters divided into two groups. The first group are steric parameters including the numbers of hydrogen atoms per site n_α, n_β and number densities of receptor sites N_α, N_β in phases α, β. Parameters from the second group define the interaction between a hydrogen atom and an absorption site including the energy parameters, which can be expressed by the pressure of half saturation P_α and P_β for phases α and β, respectively.

3.4. Result Interpretations—Microscopic Investigation of Absorption Phenomena

The effect of the increasing pressure of gaseous hydrogen on the α and β phases is presented in Figure 3.

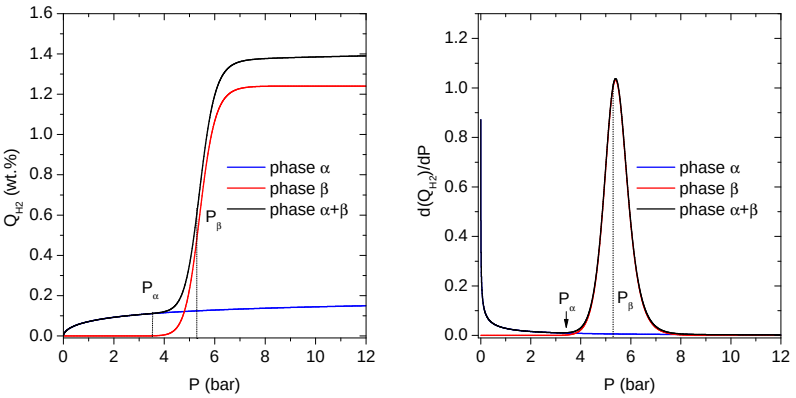

Figure 3. Evolution of the amount of absorbed hydrogen by two phases α and β as a function of increasing pressure P at T = 323 K. The computational results for the α and β phases were obtained for the first $N_1(P)$ and second components $N_2(P)$ using equation (Equation (13)). The average hydrogen amount N_a as a function of pressure is given by equation (Equation (15)).

3.4.1. Pressure Domain I: $0 < P < P_{\alpha\ sat}$

The derivative dQ_{H_2}/dP (H_2 wt.%/bar), which represents the differential amount of absorbed hydrogen per pressure unit is shown in Figure 3. The existence of maxima in dQ_{H_2}/dP indicates the phase formation. For both $LaNi_5$ and $LaNi_{4.75}Pb_{0.25}$ alloys, maxima can be observed. The first maximum, centered below 1 bar, corresponds to the α phase formation, and the second maximum, at much higher pressure, is related to the β phase formation.

Starting from zero pressure up to $P_{\alpha sat}$, the site occupancy by hydrogen atoms and α phase abundance grow as a result of the increasing hydrogen pressure surrounding the alloy. The abundance of the α phase rises intensively at low H pressures (below 0.9 bar); then the growth slows down until the saturation state is reached at $P_{\alpha sat}$ (Figure 3).

This behaviour is similar for both compounds, and it can be explained by the fact that the majority of the α phase sites are empty at the beginning of the process. Because of that, the absorption energy of the first absorption site is enough to dissociate a hydrogen molecule in contact with the alloy interface, and then to physisorb H-atoms onto the alloy surface. After physisorption, H-atoms can diffuse into the bulk of the alloy [12], and easily occupy the most energetically preferred interstitial sites of the α phase, even at a very low pressure.

The increasing hydrogen occupancy of the interstitial sites causes reduction in the number of available empty sites and slowing down of the whole absorption process. It is clearly visible as a characteristic "phase plateau" over the pressure P_α. Finally, the limit of the hydrogen capacity of the α phase is reached at pressure of $P_{\alpha sat}$. At pressure interval below $P_{\alpha sat}$ the second term of β phase is almost null (Figure 3).

3.4.2. Pressure Domain II: $P_{\alpha sat} < P < P_{\beta sat}$

The growing hydrogen pressure causes saturation of the α phase sites. Hydrogen atoms can then aggregate on the second type of sites, leading to the formation of the second hydride phase, the β phase. The peak indicating the formation of the β phase is spread out between $P_{\alpha sat}$ and $P_{\beta_s at}$ and centered around 5.4 bar for the base $LaNi_5$ alloy. The new phase is much richer in hydrogen and has a larger storage capacity with respect to the α phase (Figure 3).

The development of the β phase is characterized by a relatively high number n_β of the absorbed hydrogen atoms at the beginning of the process. The hydride β phase is also characterized by a lower density of the sites N_β as compared to N_α for the α phase. Increasing the pressure up to $P_{\beta sat}$ enables further growth of the hydrogen concentration c in the β phase, while the saturation of the α phase is maintained. An experimental manifestation of this fact in the measurement data is a characteristic two—phase region (α + β) called "plateau" on the pcT curve (Figures 1 and 2), fulfilling the Gibbs phase rule. The elevated hydrogen concentration in the alloy implies a significant H–H and M–H interaction in the β sites, leading to the lattice expansion.

3.4.3. Pressure Domain III: $P > P_{\beta sat}$

Above the saturation plateau at $P > P_{\beta sat}$, the hydride consists of the α and β phases (Figure 3). At pressures higher than $P_{\beta sat}$, the metal (alloy) hydride cannot absorb more hydrogen. In this pressure range the coexistence of two phases is observed with the abundance of 10% to 90% for α and β, respectively. Moreover, the dQ_{H_2}/dP derivative does not show any peak at $P > P_{\beta sat}$, which can be explained as the absence of any phases other than α or β.

3.4.4. Study of the Model Parameters: n_α and n_β

Figure 4 shows the evolution of the number of H-atoms per site (n_α, n_β) with temperature.

The study of n_α and n_β parameter values allows one to deduce about two potential ways the absorbed atom can be anchoraged. The first manner, where both n_α and n_β take values lower than unity, is based on multianchorage. In this type of storage, the hydrogen atom can be anchored at many neighborhood sites or some numbers of available sites are occupied by exactly one hydrogen atom—leaving the rest of sites empty. The second manner is based on a multiatom anchorage when the number of atoms per site n_α or n_β is greater than one (n_α, $n_\beta > 1$). This kind of anchoring occurs in situations where a particular interstitial site can contain more than one hydrogen atom [7]. The temperature variations of the number n_α and n_β of H-atoms per site for $LaNi_5$, and $LaNi_{4.75}Pb_{0.25}$ are collected in Figure 4. For the base alloy at 323K, n_α and n_β take the values 0.59 and 17.99, respectively. It can be therefore concluded that H-atoms in $LaNi_5$ are stored by multianchorage in the α phase and multiatom anchorage in the β phase. The different situation is observed in $LaNi_{4.75}Pb_{0.25}$, where n_α, n_β have values greater than unity. Hence it can be concluded that

rather the multiatom anchorage occurs in both phases. The above difference in H-atoms anchorage is a result of the larger unit cell for $LaNi_{4.75}Pb_{0.25}$ than $LaNi_5$.

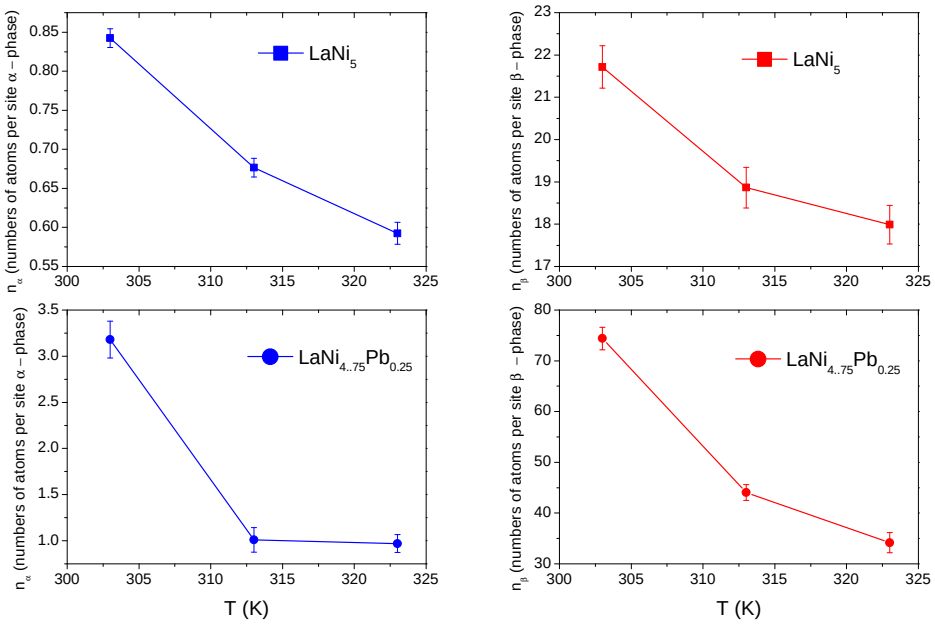

Figure 4. The temperature evolution of the number of H-atoms per receptor site n_α, n_β.

The larger unit cell results in a larger volume of the absorption sites and allows the aggregation of H-atoms, while fulfilling the Westlake [13] and Switendick [14] criteria at the same time. The first criterion assumes that minimum radius of a site has to be over 0.4 Å, but the second one takes into account the minimum distance between two hydrogen atoms that should be greater than 2.1 Å.

The n_β parameter attains values from 21.71 to 17.98 for $LaNi_5$, and 74.40 to 34.17 for $LaNi_{4.75}Pb_{0.25}$ at temperatures of 303 K and 323 K. A larger value of n_β in both compounds indicates that the β phase sites are more capacious than the α phase sites at the same temperature. For the $LaNi_5$ alloy, the n_α value is almost constant for the studied temperatures, in contrast to $LaNi_{4.75}Pb_{0.25}$, where n_α is more temperature-sensitive. For both alloys $LaNi_5$ and $LaNi_{4.75}Pb_{0.25}$, a decreasing trend in the number of H-atoms per site is observed, and this phenomenon is much stronger for the Pb-doped alloy.

The decreasing trend in the number of atoms per site is probably a consequence of two effects. The first one is the collisions between thermally activated disanchored hydrogen atoms with previous aggregates, the second effect includes the lattice expansion as a result of the rising interatomic distances during the formation the β phase.

3.4.5. Study of the Model Parameters: N_α and N_β

The parameters N_α and N_β refer to the number densities of available receptor sites per alloy unit volume. The temperature evolution of the density of the still available interstitial sites (N_α and N_β) is shown in Figure 5. The α phase receptor site density N_α is higher than N_β in the β phase for both alloys. The occupied number of receptor sites N_α and N_β increases with the increasing temperature, but with different dynamics—significantly for N_α and slightly for N_β. This is probably caused by the grain decrepitation phenomenon, through the expansion of lattice of the α phase and in consequences opening of the new available H-atoms receptor sites [12].

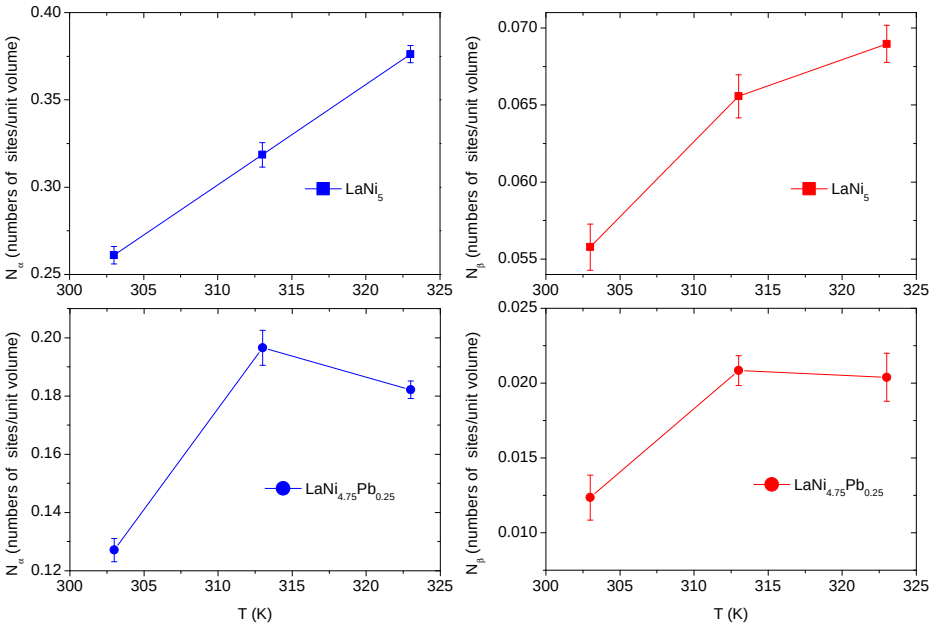

Figure 5. The temperature evolution of the number of the still available receptor sites N_α, N_β.

3.4.6. Study the Energy Parameters: Absorption Energies

The absorption energies ΔE_α and ΔE_β are calculated using values of the energy parameters P_α, P_β—fitted parameters from Model 2 and saturated vapor pressure P_{vs} of the gaseous hydrogen. The ΔE_α and ΔE_β values are given by Equations (16) and (17) [4–8] :

$$\Delta E_\alpha = RT \ln\left(\frac{P_{vs}}{P_\alpha}\right), \tag{16}$$

$$\Delta E_\beta = RT \ln\left(\frac{P_{vs}}{P_\beta}\right), \tag{17}$$

where R is the ideal gas constant, $R = 8.314472$ J/mol K and P_{vs} is given by Equation (18) [4–8]:

$$P_{vs} = \exp\left[12.69 - \frac{94.896}{T} + (1.1125)\ln(T) + (3.2915 \cdot 10^{-4})\, T^2\right]. \tag{18}$$

The absorption energies ΔE_α and ΔE_β characterize the types of binding between hydrogen atoms and a host alloy sites in the phases α and β, respectively. The temperature evolution of the absorption energies ΔE_α and ΔE_β for $LaNi_5$ and $LaNi_{4.75}Pb_{0.25}$ are presented in Figure 6 and in Table 4. The absorption energy values obtained for $LaNi_{4.75}Pb_{0.25}$ are close to those obtained for the nondoped alloy $LaNi_5$, and they take values of over 100 kJ/mol in both cases. Hence it can be assumed that, for all investigated alloys, H-atoms are chemisorbed on the host alloys sites by creating metallic bonding, which are chemical in their nature. Moreover, in case of both compounds the relation $\Delta E_\alpha < \Delta E_\beta$ is preserved. The values obtained for the hydrides of alloys $LaNi_5$ and $LaNi_{4.75}Pb_{0.25}$ are comparable and consistent with values reported by other researchers for different hydrides of $LaNi_{5-x}M_x$ type alloys. For example, in hydride $LaNi_{4.6}Al_{0.4}$, whose results are reported in [6], at temperatures 303 K and 313 K, absorption energies ΔE_α at α phase are 124.75 kJ/mol and 121.95 kJ/mol respectively. Similarly, for β phase, ΔE_β takes the values 133.64 kJ/mol and 131.08 kJ/mol at the above temperatures.

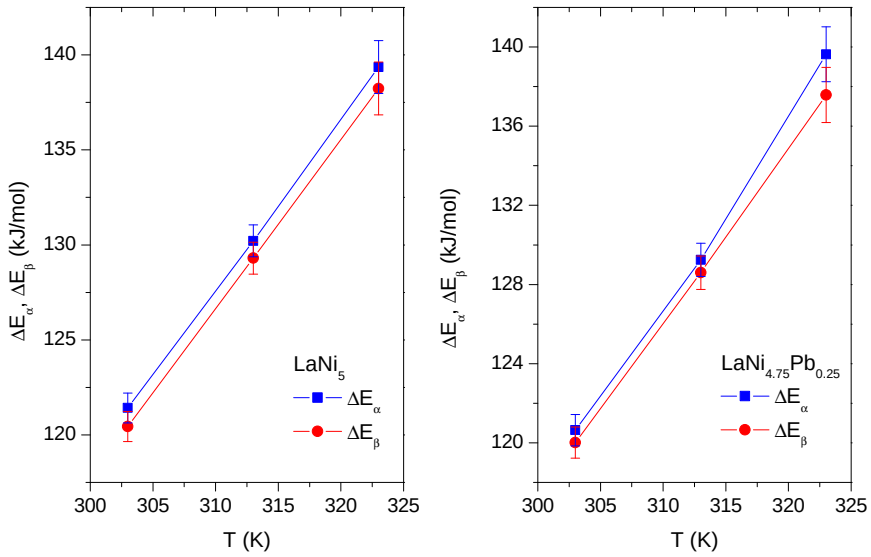

Figure 6. The absorption energies ΔE_α and ΔE_β versus temperature.

Table 4. Values of the absorption energies ΔE_α and ΔE_β for both investigated alloys versus the process temperature.

Alloy	Temp (K)	ΔE_α (kJ/mol)	ΔE_β (kJ/mol)
$LaNi_5$	303	121.4	120.4
	313	130.2	129.3
	323	139.5	138.2
$LaNi_{4.75}Pb_{0.25}$	303	120.0	120.4
	313	129.3	128.9
	323	138.7	137.9

For hydrides of $LaNi_5$ and $LaNi_{4.75}Pb_{0.25}$, the increasing values of energies ΔE_α, ΔE_β with the increasing temperature are observed. This behavior can be explained by the effect of thermal agitation. Thus, the sites have higher energies at growing temperature, which makes it more difficult to penetrate those volumes by hydrogen atoms. As a consequence, a greater pressure (energy) is required to deposit the H-atom at the same site. Thus, the absorption energy increases with increasing temperature (Figure 6).

3.4.7. Investigation of Internal Energy

Internal energy E_{int} exists as a sum of all forms of energy stored in the system, including actual interactions between the gas–gas particles and gas–alloy receptor site. The internal energy E_{int} is given by Equation (19) [4–8]:

$$E_{int} = -\frac{\partial \ln Z_g}{\partial \beta} + \frac{\mu}{\beta}\left(\frac{\partial \ln Z_g}{\partial \mu}\right). \quad (19)$$

Equation (19) for internal energy E_{int} can be further written as the following expression:

$$E_{int} = k_B T \ln \frac{\beta P}{Z_g}\left(\frac{N_\alpha \left(\frac{P}{P_\alpha}\right)^{n_\alpha}}{1+\left(\frac{P}{P_\alpha}\right)^{n_\alpha}} + \frac{N_\beta \left(\frac{P}{P_\beta}\right)^{n_\beta}}{1+\left(\frac{P}{P_\beta}\right)^{n_\beta}}\right) - k_B T \ln \frac{\beta P}{Z_g}\left(\frac{N_\alpha \left(\frac{P}{P_\alpha}\right)^{n_\alpha} \ln\left(\frac{P}{P_\alpha}\right)^{n_\alpha}}{1+\left(\frac{P}{P_\alpha}\right)^{n_\alpha}} + \frac{N_\beta \left(\frac{P}{P_\beta}\right)^{n_\beta} \ln\left(\frac{P}{P_\beta}\right)^{n_\beta}}{1+\left(\frac{P}{P_\beta}\right)^{n_\beta}}\right). \quad (20)$$

Thus, Equation (20) can be divided into two additive contributions, given by Equations (21) and (22), originating from the first and second type sites from the α and β phases, which represent different absorption levels.

$$E_{int\alpha} = k_B T \ln \frac{\beta P}{Z_g} \left(\frac{N_\alpha \left(\frac{P}{P_\alpha}\right)^{n_\alpha}}{1 + \left(\frac{P}{P_\alpha}\right)^{n_\alpha}} \right) - k_B T \left(\frac{N_\alpha \left(\frac{P}{P_\alpha}\right)^{n_\alpha} \ln \left(\frac{P}{P_\alpha}\right)^{n_\alpha}}{1 + \left(\frac{P}{P_\alpha}\right)^{n_\alpha}} \right), \quad (21)$$

$$E_{int\beta} = k_B T \ln \frac{\beta P}{Z_g} \left(\frac{N_\beta \left(\frac{P}{P_\beta}\right)^{n_\beta}}{1 + \left(\frac{P}{P_\beta}\right)^{n_\beta}} \right) - k_B T \left(\frac{N_\beta \left(\frac{P}{P_\beta}\right)^{n_\beta} \ln \left(\frac{P}{P_\beta}\right)^{n_\beta}}{1 + \left(\frac{P}{P_\beta}\right)^{n_\beta}} \right). \quad (22)$$

The results of the internal energy E_{int} computation are presented in Figure 7.

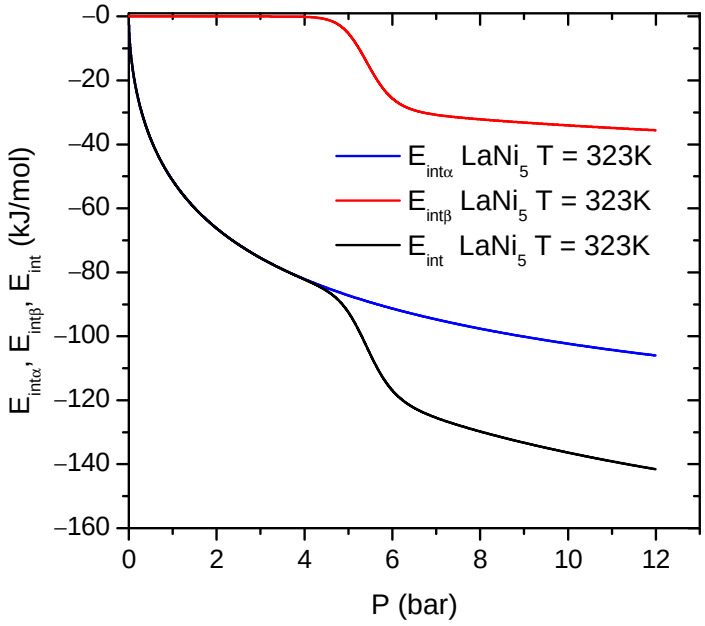

Figure 7. Evolution of the absorption internal energy of the first (Equation (21)) and second site (Equation (22)) and the overall energy versus pressure for T = 323 K presented only for $LaNi_5$ (Equation (20)). The similar energy evolution is observed for $LaNi_{4.75}Pb_{0.25}$.

At the beginning of the process (0 bar pressure), the internal energy is null. Increasing pressure leads to nonzero values of the internal energy and it then further algebraically decreases. During the whole hydrogen absorption process, the internal energy remains negative, with a step centered at the pressure of the β phase formation. The negative internal energy values are a manifestation of the exothermic nature of the absorption process and the release of energy to the environment. At a pressure below that of the α phase site saturation, the energy contribution $E_{a\beta}$ related to the second type site is rather constant and takes values close to zero. Increasing the pressure above $P_{\alpha sat}$ causes a step change in $E_{a\beta}$ (Figure 7). Moreover, the contribution to E_{int} from the α phase shows a higher energy dissipation during absorption compared to the β phase. The temperature evolution of the internal energy E_{int} versus pressure at the two absorption temperatures T = 303 K and 323 K for $LaNi_5$ and $LaNi_{4.75}Pb_{0.25}$ is presented in Figure 8. At a fixed pressure, the total absolute E_{int} values are greater for $LaNi_5$ than for $LaNi_{4.75}Pb_{0.25}$. The absorption process for $LaNi_5$ is more energetic that for the nondoped alloy, as it requires or releases more energy (heat) during absorption/desorption process than for $LaNi_{4.75}Pb_{0.25}$ (Figure 8).

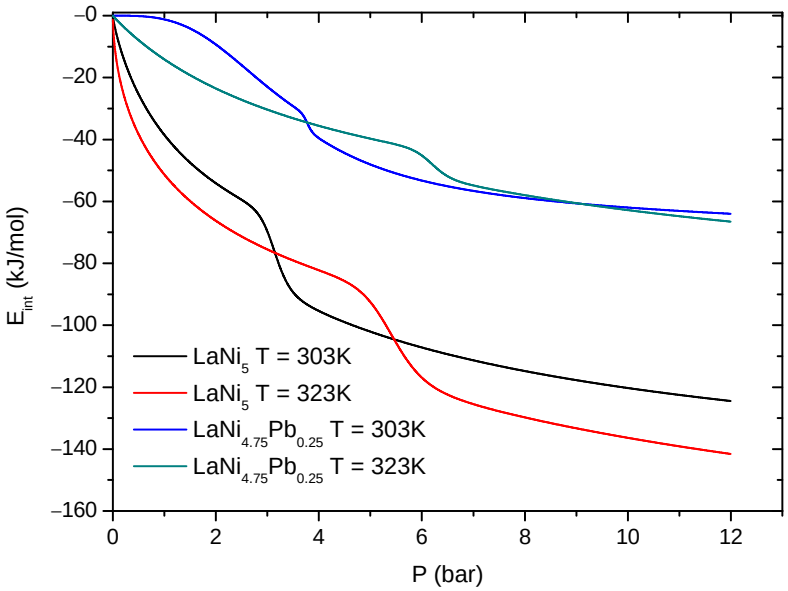

Figure 8. Evolution of the internal energy E_{int} (Equation (20)) as a function of pressure for the absorption process for $LaNi_5$ and $LaNi_{4.75}Pb_{0.25}$ at T = 303 K and T = 323 K.

3.4.8. Investigation of the Gibbs Free Energy

The Gibbs free energy G_a is one of the thermodynamic functions, which gives information about the spontaneity of the system and its interaction with external environment. The definition of G_a is given by Equation (23) [4–6,15]:

$$G_a = \mu_m N_a, \tag{23}$$

where N_a is the absorbed quantity of hydrogen and μ_m is the chemical potential from Equation (8). Finally G_a can be written as Equation (24):

$$G_a = k_B T \ln \frac{\beta P}{Z_g} \left(\frac{n_\alpha N_\alpha}{1 + \left(\frac{P_\alpha}{P}\right)^{n_\alpha}} + \frac{n_\beta N_\beta}{1 + \left(\frac{P_\beta}{P}\right)^{n_\beta}} \right). \tag{24}$$

Similarly as for the internal energy E_{int}, there are two contributions to the overall Gibbs free energy G_a, related to the absorption sites of two types from the α and β phases. Each contribution can be expressed by Equations (25) and (26).

$$G_{a\alpha} = k_B T \ln \frac{\beta P}{Z_g} \left(\frac{n_\alpha N_\alpha}{1 + \left(\frac{P_\alpha}{P}\right)^{n_\alpha}} \right), \tag{25}$$

$$G_{a\beta} = k_B T \ln \frac{\beta P}{Z_g} \left(\frac{n_\alpha N_\beta}{1 + \left(\frac{P_\beta}{P}\right)^{n_\beta}} \right). \tag{26}$$

Figure 9 illustrates the evolution of the Gibbs free energy during the hydrogen absorption process for $LaNi_5$. The general discussion will be done on the example of $LaNi_5$. From Figure 9, it can be noticed that the Gibbs free energy takes nonzero values first for the α phase. At pressure above $P_{\alpha sat}$ (saturation of the α sites), $G_{a\alpha}$ is almost constant and the absorption process at the α phase sites loses its previous spontaneity. At the same pressure range, the $G_{a\beta}$ free energy contribution becomes significant. However, the Gibbs free energy $G_{a\beta}$ related to the second phase site takes lower values, therefore it can be concluded that the H-atoms absorption process is much more spontaneous for the β phase

than for the α phase. The α phase sites are much more energetic than the β phase sites, which reflects in higher absorption energies (Figure 6 and Table 4).

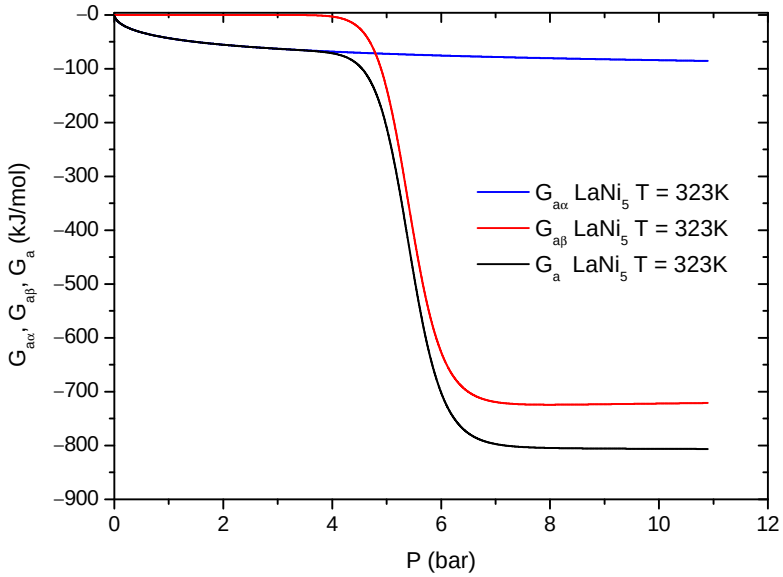

Figure 9. Evolution of the Gibbs free energy G_a of the first (Equation (25)) and second sites (Equation (26)), and the overall G_a (Equation (24)) versus pressure for $LaNi_5$ at T = 323 K.

The Gibbs free energy values in the high pressure range are negative. Hence, absorption phenomena are spontaneous in their nature. At a fixed pressure and increasing temperature, the values of total G_a increase algebraically and decrease in absolute value. This suggests that the whole absorption process becomes less spontaneous at elevated temperatures. Consequently, it leads to the decrease in the amount of the absorbed hydrogen with increasing temperature. From Figure 10 it can be seen that, for the base alloy $LaNi_5$ at a fixed pressure, the absolute values of the Gibbs energy are greater than for $LaNi_{4.75}Pb_{0.25}$, which indicates that for the nondoped alloy, the H absorption process is much more spontaneous.

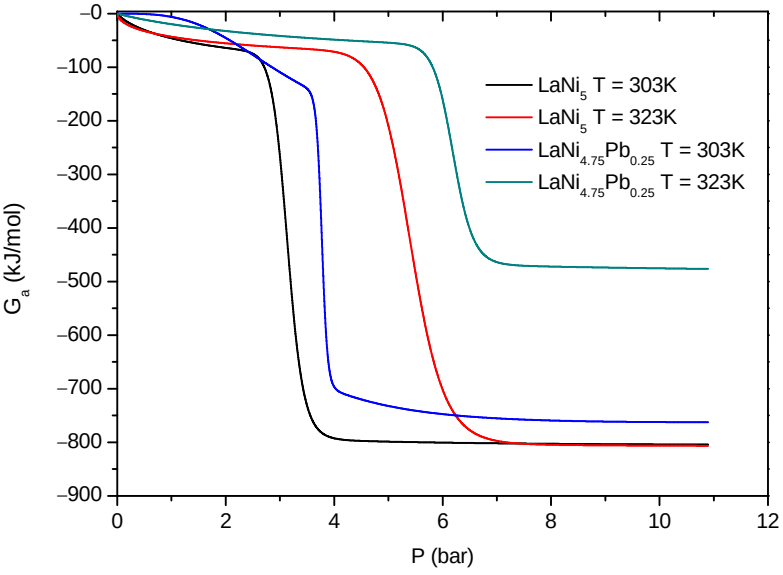

Figure 10. Evolution of the Gibbs free energy G_a of absorption versus pressure for $LaNi_5$ and $LaNi_{4.75}Pb_{0.25}$ at T = 303 K and T = 323 K (Equation (24)).

3.4.9. Investigation of the Entropy

The entropy evolution during the hydrogen absorption process provides information about the homogeneity level of the system and its degree of disorder. Hence, the entropy can be also identified as an indicator of the process spontaneity. The entropy is determined through the grand potential J and the grand canonical partition function Z_{gc} of the system by Equation (27) [4,5,7,8]:

$$J = -k_B T \ln Z_g. \tag{27}$$

Since the grand potential J is defined as $J = E_{int} - \mu N - T$ [4,5,7]:

$$J = -\frac{\partial \ln Z_g}{\partial \beta} - TS_a, \tag{28}$$

using Equations (27) and (28), the entropy can be expressed in a simple form:

$$TS_a = -\frac{\partial \ln Z_g}{\partial \beta} + k_B T \ln Z_g, \tag{29}$$

$$\frac{S_a}{k_B} = -\beta \frac{\partial \ln Z_g}{\partial \beta} + \ln Z_{gc}. \tag{30}$$

Finally, by substituting and performing algebraic operations with Equation (30), it is possible to obtain Equation (31) for entropy S_a:

$$\begin{aligned} S_a = k_B & \left(N_\alpha \ln \left(1 + \frac{P}{P_\alpha} \right)^{n_\alpha} + N_\beta \ln \left(1 + \frac{P}{P_\beta} \right)^{n_\beta} \right) \\ - k_B & \left(\frac{N_\alpha \left(\frac{P}{P_\alpha} \right)^{n_\alpha} \ln \left(\frac{P}{P_\alpha} \right)^{n_\alpha}}{1 + \left(\frac{P}{P_\alpha} \right)^{n_\alpha}} + \frac{N_\beta \left(\frac{P}{P_\beta} \right)^{n_\beta} \ln \left(\frac{P}{P_\beta} \right)^{n_\beta}}{1 + \left(\frac{P}{P_\beta} \right)^{n_\alpha}} \right). \end{aligned} \tag{31}$$

Similarly as for the internal energy E_{int}, Equation (20) or free enthalpy G_a, Equation (24), the entropy consists of two contributions $S_{a\alpha,\beta}$ related to the first and second site types in the α and β phases. These entropy contributions $S_{a_\alpha,\beta}$ are described by Equations (32) and (33).

$$S_{a\alpha} = k_B \left(N_\alpha \ln \left(1 + \frac{P}{P_\alpha} \right)^{n_\alpha} - \left(\frac{N_\alpha \left(\frac{P}{P_\alpha} \right)^{n_\alpha} \ln \left(\frac{P}{P_\alpha} \right)^{n_\alpha}}{1 + \left(\frac{P}{P_\alpha} \right)^{n_\alpha}} \right) \right), \tag{32}$$

$$S_{a\beta} = k_B \left(N_\beta \ln \left(1 + \frac{P}{P_\beta} \right)^{n_\beta} - \left(\frac{N_\beta \left(\frac{P}{P_\beta} \right)^{n_\beta} \ln \left(\frac{P}{P_\beta} \right)^{n_\beta}}{1 + \left(\frac{P}{P_\beta} \right)^{n_\beta}} \right) \right). \tag{33}$$

The evolution of the entropy versus pressure of the $LaNi_5$ hydride is presented in Figure 11. It can be clearly seen that the entropy has two maxima corresponding to the pressure of the α and β phase formation, as contributions to the overall entropy. Similar situation is observed for the Pb-doped alloy, so the general discussion is done only for the base alloy.

The entropy S_a shows different behavior below and above the half saturation pressures P_α and P_β. Starting from the low pressure, the entropy $S_{a\alpha}$ related to the α phase reaches a local maximum at the pressure of half saturation (at $P = P_\alpha$). It is an effect of a step change in the system disorder caused by the intensive movements of hydrogen atoms around pressure P_α, which corresponds to the greatest reactivity. Further increasing of pressure, $P > P_\alpha$, causes an increase of the hydrogen concentration and reduction of the number of the empty α sites, until the full α sites saturation is reached. As a result of the increasing

saturation of the α sites, the configuration disorder disappears. This phenomenon is visible in the $S_{a\alpha}$ values approaching zero above the half saturation pressure P_α. The second maximum $S_{a\beta}$ is reached at the pressure P_β, corresponding to half saturation of the β phase. Beyond the second half saturation P_β, H-atoms have a lower probability to select free receptor sites, so the entropy expressed by $S_{a\beta}$ decreases. When the saturation is attained for both phases α and β, their disorder decreases to zero (Figure 12).

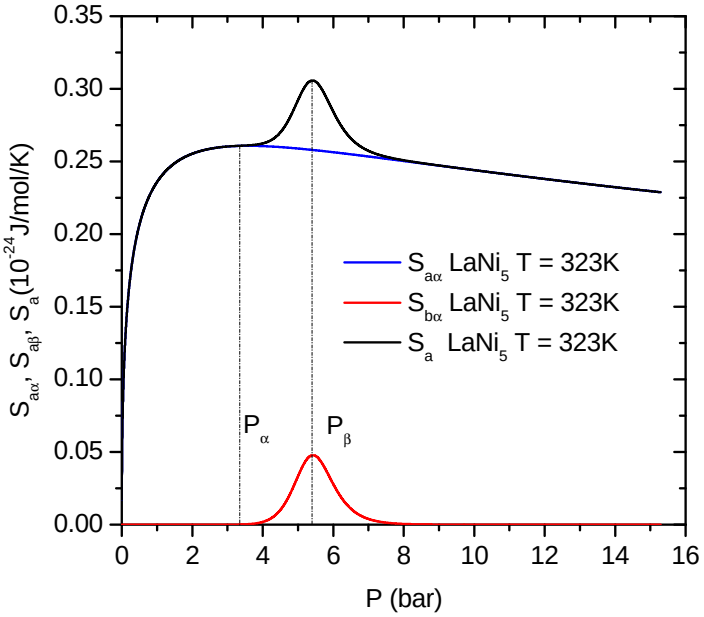

Figure 11. Evolution of the absorption entropy of the α phase (Equation (32)), the β phase (Equation (33)) and the overall according to the pressure at T = 323 K (Equation (31)).

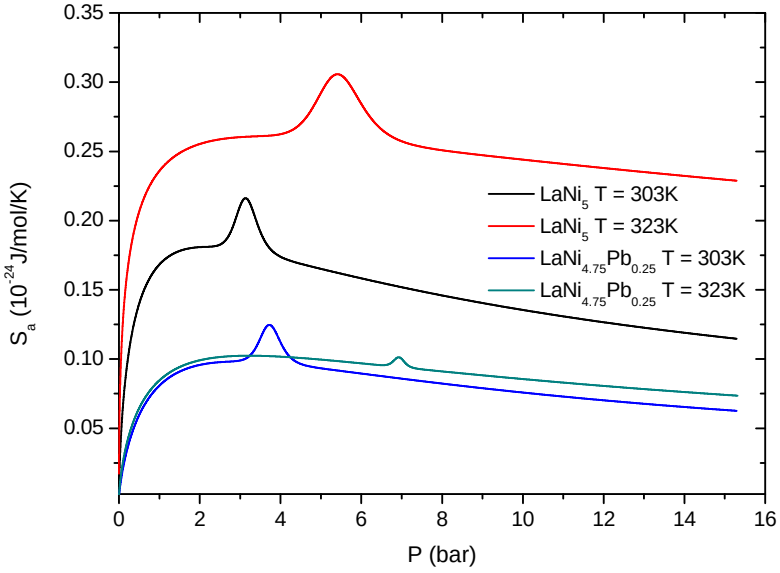

Figure 12. Evolution of the overall absorption entropy versus pressure at T = 303 K, T = 323 K for $LaNi_5$ and $LaNi_{4.75}Pb_{0.25}$ (Equation (31)).

4. Conclusions

The statistical physics formalism based on the grand canonical ensemble with some simplifying hypotheses was applied to describe the hydrogen absorption processes in alloys $LaNi_5$ and $LaNi_{4.75}Pb_{0.25}$ at a microscopic level. The tested model is thermodynamically coherent and the physicochemical parameters showed by the absorption process are taken

into consideration in the theoretical method. The hydrogen absorption in the $LaNi_5$ and $LaNi_{4.75}Pb_{0.25}$ alloys is a chemisorption with two energy levels, which are supposed to correspond to the α and β phases. The parameters n_α and n_β corresponding to the α and β phases are dissimilar in values. The first one is close to 1 for the hydride of $LaNi_5$ and about 3 for the hydride of $LaNi_{4.75}Pb_{0.25}$. The second parameters n_β is much higher than the first one. The difference between alloys explained by the differences between the unit cell volumes, which is bigger in doped alloy than in the base alloy. The parameters N_α and N_β increase with growing temperature. The influence of thermal agitation becomes evidenced in this way. Thermal agitation hampers hydrogen atoms anchoring and disanchors the absorbed atoms. An energetic study has been carried out by means of the parameters P_α and P_β deduced from the model curve fits to the experimental data. The values of absorption energies ΔE_α and ΔE_β (>100 kJ/mol) indicated that, for both hydrides of tested alloys, hydrogen was chemically absorbed. These energies increased with temperature. Moreover, it was shown that the Pb-doping of the base $LaNi_5$ alloy caused changes in the microscopic state of the alloy. As a consequence, the reduction of absorption spontaneity was evidenced from the course of the Gibbs enthalpy. The internal energy and entropy change during the hydrogen absorption process. It can be finally concluded that the applied statistical physics model proved correct and capable of plausibly interpreting the experimental isotherms, as well as deriving consistent and meaningful physical parameters.

Author Contributions: Conceptualization, M.Ż. and W.Z.; methodology, M.Ż. and W.Z.; investigation, M.Ż.; data curation, M.Ż.; writing—original draft preparation, M.Ż.; writing—review and editing, W.Z.; supervision, W.Z. All authors have read and agreed to the published version of the manuscript.

Funding: EU Project POWR.03.02.00-00-I004/16.

Data Availability Statement: Data are contained within the article.

Conflicts of Interest: The authors declare no conflict of interest.

Abbreviations

T	temperature (K)
n	stoichiometric coefficient representing the number of H-atoms absorbed during reaction
N_a	number of hydrogen atoms absorbed
N_M	number of interstitial sites located in the unit mass of a hydride
Z_{gc}	grand canonical partition function
$\epsilon_{\alpha\,\beta}$	absorption energy per site in (kJ/mol)
k_B	Boltzmann constant equal $1.38064{\cdot}10^{-23}$ J/K
μ, μ_m	chemical potential of a hydrogen absorption site
N_1, N_2	numbers of hydrogen atoms absorbed in two independent kinds of interstitial sites
α, β	names of existing phases connecting to different hydrogen occupations levels
n_α, n_β	numbers of hydrogen atoms absorbed in two independent kinds of interstitial sites
N_α, N_β	number densities of interstitial sites (number of such sites per unit volume of the alloy)
P_α, P_β	the pressure according to half of hydrogen capacity saturation in α and β phases
$P_{\alpha sat}, P_{\beta sat}$	the pressure according of full phases hydrogen capacity saturation in α and β phases
P_{vs}	hydrogen saturated vapor pressure (Pa)
$\Delta E_\alpha, \Delta E_\beta$	hydrogen absorption energies in α and β phases (kJ/mol)
$E_{int}, E_{int\alpha}, E_{int\beta}$	internal energy and two additive contributions become from α and β phases (J/mol)
$G_a, G_{a\alpha}, G_{a\beta}$	free enthalpy and two additive contributions become from α and β phases (kJ/mol)
$S_a, S_{a\alpha}, S_{a\beta}$	entropy and two additive contributions become from α and β phases (J/mol/K)

References

1. Senoh, H.; Kiyobayashi, T. Hydrogenation and Dehydrogenation Properties of $RHNi_5$ (RH = Heavy Rare Earth) Binary Intermetallic Compounds. *Mater. Trans.* **2004**, *45*, 292–295. [CrossRef]
2. Senoh, H.; Kiyobayashi1, T. Hydrogenation Properties of RNi_5 (R: Rare Earth) Intermetallic Compounds with Multi Pressure Plateaux. *Mater. Trans.* **2003**, *44*, 1663–1666. [CrossRef]
3. Łodziana, Z. Ternary $LaNi_{4.75}M_{0.25}$ hydrogen storage alloys: Surface segregation, hydrogen sorption and thermodynamic stability. *Int. J. Hydrogen Energy* **2018**, *44*, 1760–1773. [CrossRef]
4. Bouaziz, N. Physicochemical and thermodynamic investigation of hydrogen absorption and desorption in $LaNi_{3.8}Al_{1.0}Mn_{0.2}$ using the statistical physics modeling. *Results Phys.* **2018**, *9*, 1323–1334. [CrossRef]
5. Bouaziz, N. Theoretical study of hydrogen absorption-desorption on $LaNi_{3.8}Al_{1.2-x}Mn_x$ using statistical physics treatment. *Phys. B* **2017**, *525*, 46–59. [CrossRef]
6. Bouaziz, N. Statistical physics modeling of hydrogen absorption onto $LaNi_{4.6}Al_{0.4}$: Stereographic and energetic interpretations. *Sep. Sci. Technol.* **2019**, *414*,170–181. [CrossRef]
7. Wjihi, S. P-C isotherms of $LaNi_{4.75}Fe_{0.25}$ alloy at different temperatures statistical physics modeling of hydrogen sorption onto $LaNi_{4.75}Fe_{0.25}$. Microscopic interpretation and thermodynamic potential investigation. *Fluid Phase Equilibria* **2016**, *414*, 170–181. [CrossRef]
8. Khalfaoui, M. Modeling and interpretations by the statistical physics formalism of hydrogen adsorption isotherm on $LaNi_{4.75}Fe_{0.25}$. *Int. J. Hydrogen Energy* **2013**, *38*, 11536–11542.
9. Sellaoui, L.; Depci, T. A new statistical physics model to interpret the binary adsorption isotherms of lead and zinc on activated carbon. *J. Mol. Liq.* 2015, *in press*.
10. Mechi, N. A macroscopic investigation to interpret the absorption and desorption of hydrogen in $LaNi_{4.85}Al_{0.15}$ alloy using the grand canonical ensemble. *Fluid Phase Equilibria* 2016, *in press*.
11. Yu, B.; Rumer, M.; Ryvkin, S. *Thermodynamics, Statistical Physics, and Kinetics*; Mir Publishers Moscow, USSR: Moscow, Russia, 1980; ISBN 082851853X.
12. Leblond, J.B. A general mathematical description of hydrogen diffusion in steels. Derivation of diffusion equations from Boltzmann-type transport equations. *Acta Met.* **1983**, *31*, 1459–1469. [CrossRef]
13. Westlake, D.G. Site occupancies and stoichiometries in hydrides of intermetallic compounds: Geometric considerations. *J. Less Common Met.* **1983**, *90*, 251–273. [CrossRef]
14. Switendick, A.C. Band structure calculations for metal hydrogen systems. *Z. fur Phys. Chem.* **1979**, *117*, 89–112. [CrossRef]
15. Knani, S. Modeling of the psychophysical response curves using the grand canonical ensemble in statistical physics. *Food Biophys.* **2007**, *2*, 183–192. [CrossRef]